



Application of Weighted Gene Co-expression Network Analysis for Data from Paired Design

Citation

Li, Jianqiang, Doudou Zhou, Weiliang Qiu, Yuliang Shi, Ji-Jiang Yang, Shi Chen, Qing Wang, and Hui Pan. 2018. "Application of Weighted Gene Co-expression Network Analysis for Data from Paired Design." *Scientific Reports* 8 (1): 622. doi:10.1038/s41598-017-18705-z. <http://dx.doi.org/10.1038/s41598-017-18705-z>.

Published Version

doi:10.1038/s41598-017-18705-z

Permanent link

<http://nrs.harvard.edu/urn-3:HUL.InstRepos:34868835>

Terms of Use

This article was downloaded from Harvard University's DASH repository, and is made available under the terms and conditions applicable to Other Posted Material, as set forth at <http://nrs.harvard.edu/urn-3:HUL.InstRepos:dash.current.terms-of-use#LAA>

Share Your Story

The Harvard community has made this article openly available.
Please share how this access benefits you. [Submit a story](#).

[Accessibility](#)

SCIENTIFIC REPORTS



OPEN

Application of Weighted Gene Co-expression Network Analysis for Data from Paired Design

Jianqiang Li^{1,2}, Doudou Zhou¹, Weiliang Qiu³, Yuliang Shi^{1,2}, Ji-Jiang Yang⁴, Shi Chen⁵, Qing Wang⁴ & Hui Pan⁵

Investigating how genes jointly affect complex human diseases is important, yet challenging. The network approach (e.g., weighted gene co-expression network analysis (WGCNA)) is a powerful tool. However, genomic data usually contain substantial batch effects, which could mask true genomic signals. Paired design is a powerful tool that can reduce batch effects. However, it is currently unclear how to appropriately apply WGCNA to genomic data from paired design. In this paper, we modified the current WGCNA pipeline to analyse high-throughput genomic data from paired design. We illustrated the modified WGCNA pipeline by analysing the miRNA dataset provided by Shiah *et al.* (2014), which contains forty oral squamous cell carcinoma (OSCC) specimens and their matched non-tumourous epithelial counterparts. OSCC is the sixth most common cancer worldwide. The modified WGCNA pipeline identified two sets of novel miRNAs associated with OSCC, in addition to the existing miRNAs reported by Shiah *et al.* (2014). Thus, this work will be of great interest to readers of various scientific disciplines, in particular, genetic and genomic scientists as well as medical scientists working on cancer.

Genetics plays an important role in the aetiologies of many complex human diseases. Genes are functional units of genetic materials. It is believed that whether a gene is expressed or not affects the synthesis of downstream proteins, which are the building blocks of the human body. However, recent studies have shown that individual genes do not work alone. Instead, genes interact with each other and jointly affect human health. Studies have shown that each gene is estimated on average to interact with four to eight other genes¹ and to be involved in 10 biological functions². Gene networks provide the potential to identify hundreds of genes that are associated with complex human diseases and that could serve as points for therapeutic interventions^{3,4}, and this information is important for predicting the functions of new genes and finding genes that play key roles in complex human diseases. Constructing a gene co-expression network (GCN) is an effective way to characterize the correlation patterns among genes. Densely connected sub-networks form gene modules, which are usually related to biological functions. A gene co-expression network is an undirected graph, where each node corresponds to a gene, and each edge connects a pair of genes that are significantly correlated⁵.

Weighted gene co-expression network analysis (WGCNA)⁶ is a popular systems biology method used to not only construct gene networks but also detect gene modules and identify the central players (i.e., hub genes) within modules. The WGCNA pipeline is as follows: 1. Construct a gene co-expression network represented mathematically by an adjacency matrix, the element of which indicates co-expression similarity between a pair of genes. 2. Identify modules: WGCNA uses hierarchical clustering to identify modules. To measure the dissimilarity between clusters, WGCNA uses a topological overlap measure that can result in biologically meaningful modules in real data analysis. 3. Relate modules to phenotypes: several methods can be used to measure the association of a module to a phenotypic trait. For instance, one can test the association between the module eigengene (ME) and the phenotypic trait. The ME of a module is defined as the first principal component of the module. One can also use the module significance (MS), which is defined as the average gene significance (GS)

¹Faculty of Information Technology, Beijing University of Technology, Beijing, 100124, China. ²Beijing Engineering Research Center for IoT Software and Systems, Beijing, 100124, China. ³Channing Division of Network Medicine, Brigham and Women's Hospital/Harvard Medical School, 181 Longwood Avenue, Boston, MA, 02115, USA.

⁴Tsinghua National Laboratory for Information Science and Technology, Tsinghua University, Beijing, 100084, China.

⁵Department of Endocrinology, Peking Union Medical College Hospital, Chinese Academe of Medical Sciences & Peking Union Medical College, Beijing, 100730, China. Jianqiang Li and Doudou Zhou contributed equally to this work. Correspondence and requests for materials should be addressed to J.-J.Y. (email: jjjiangyang@126.com)

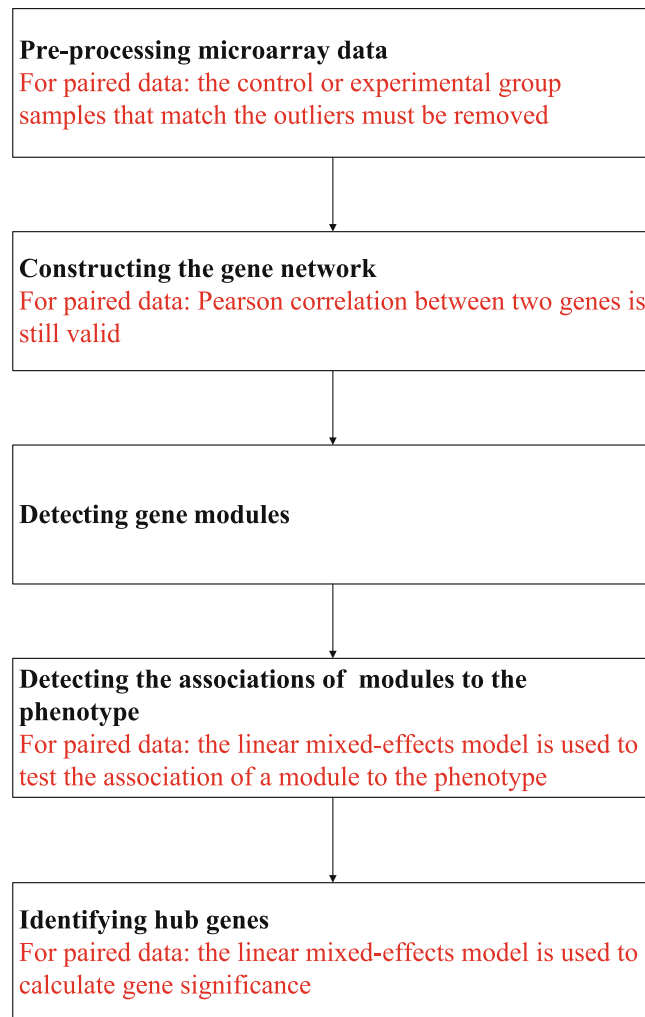


Figure 1. Flow chart of the modified WGCNA pipeline.

of all genes in the module, to assess the association of a module to a phenotype. The GS of a node is defined as the correlation between the node and the phenotypic trait. Modules with high trait significance may represent pathways associated with the phenotypic trait. 4. Study inter-module relationships: WGCNA uses ME as a representative profile of a module and quantifies module similarity by eigengene correlation. Studying the relationship of the modules can help to find which modules are highly related. 5. Find key drivers in interesting modules: the nodes having the largest number of edges are most important because the malfunction of this gene would affect all connected genes. WGCNA assumes that genetic networks obey the scale-free topology criterion. Instead of dichotomizing gene co-expression (connected = 1, unconnected = 0), WGCNA uses a 'soft' threshold to determine the weights of the edges connecting pairs of genes, which has been proven to yield more robust results than unweighted networks⁷. An appropriate soft threshold will make the resulting co-expression network closer to a scale-free network. Instead of relating individual genes to phenotype, WGCNA focuses on the relationship between a few modules and the trait, which greatly alleviates the multiple testing problem inherent in microarray data analysis⁸. WGCNA is widely used in genomic data analysis, in which samples are assumed independent of each other.

The paired design is powerful for reducing the confounding effects and has been used successfully in genomic studies. However, it is currently unclear how to appropriately apply WGCNA to genomic data from paired design. For independent data, WGCNA uses the Pearson correlation to measure the magnitude of co-expression between nodes (such as a gene or microRNA) in a network. Can we use the Pearson correlation to measure the magnitude of co-expression between two nodes for paired samples? How do we evaluate the associations of gene modules to the phenotype of interest for data from paired design? How do we calculate gene significance for data from paired design? To address these questions, we propose in this article to modify the current WGCNA pipeline. The modified pipeline can be divided into five steps, as is shown in Fig. 1. We illustrate the modified pipeline using the Gene Expression Omnibus (GEO)^{9,10} dataset (GSE45238)¹¹ to investigate the associations of microRNAs to oral squamous cell carcinomas (OSCC).

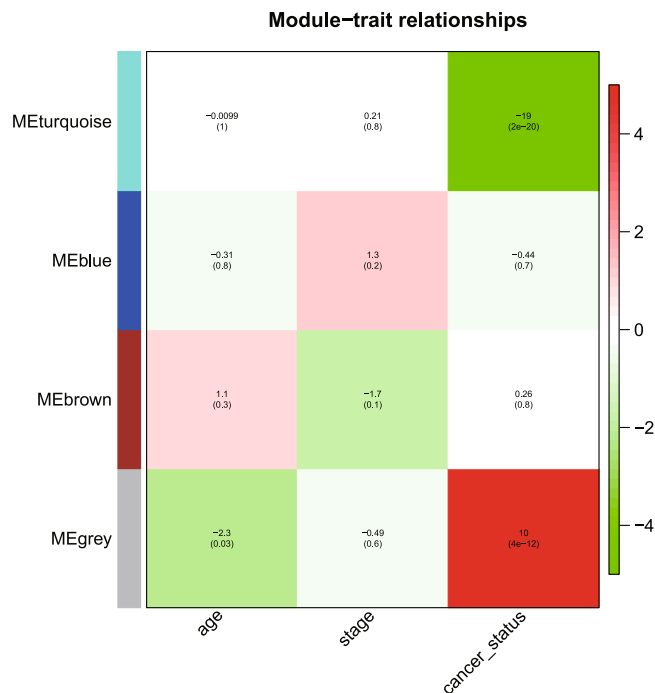


Figure 2. Module-trait association. Each row corresponds to a module; each column corresponds to a trait. Each cell contains the test statistic value and its corresponding p value from the linear mixed-effects model.

Results

In this work, we showed that (1) the Pearson correlation could be used to measure the magnitude of co-expression between two genes regardless of whether the samples are paired or independent and (2) to evaluate the associations of modules/genes to phenotypes, we need to account for the within-pair correlation by appropriate statistical models, such as the linear mixed effects model (LMM). Based on the WGCNA pipeline we modified, we identified four miRNA modules (Supplementary Fig. 9) for the OSCC data. There were 254 miRNAs in the turquoise module, 189 miRNAs in the blue module, 78 miRNAs in the brown module, and 309 miRNAs in the grey module. Some MEs are highly correlated based on the hierarchical clustering analysis (Supplementary Fig. 10). The result of the linear mixed-effects model shows that the turquoise module (t-value = -18.68, p-value = 1.97e-20) and the grey module (t-value = 10, p-value = 4e-12) are significantly associated with cancer status (see Fig. 2). We also compared the MS among the modules (see Fig. 3), and the results showed that the turquoise module had the highest relevance to cancer status.

For each miRNA in a module, we drew the module membership (MM) against the GS in a scatter plot (see Fig. 4). The module membership (MM): $MM(i) = cor(x_i, ME)$ is defined in WGCNA to measure the importance of the gene within the module. The greater the absolute value of $MM(i)$ is, the more important the gene i is in the module⁶. It can be seen that the GS in the turquoise module is highly correlated with MM, illustrating that miRNAs significantly associated with cancer status are often also the important elements of the turquoise module.

For the turquoise module, the hub is miR-let-7c, which is connected to 140 miRNAs (see Fig. 5). According to Wikipedia (https://en.wikipedia.org/wiki/Let-7_microRNA_precursor), let-7 acts as a tumour suppressor. Manikandan *et al.*¹² showed that let-7a, let-7d, and let-7f are differentially expressed in OSCC. Hui AB *et al.*¹³ showed that let-7c was down-regulated in head and neck squamous cell carcinoma (HNSCC). The turquoise module contains the two miRNAs (miR-329 and miR-410) that were identified by Shiah *et al.*¹¹. The information about miR-let-7c, miR-329 and miR-410 is listed in Table 1. Seventy-one of the 84 miRNAs detected by Shiah *et al.* are in the turquoise module and none of them are in the blue or brown modules.

We uploaded the miRNAs in the turquoise module and the grey module to miRsystem¹⁴ and obtained 9233 targets in the turquoise module and 8629 targets in the grey module. There were 7628 overlapping targets. The results showed that the top 6 enriched KEGG pathways for the two modules are the same: Pathways in Cancer, mapk Signalling Pathway, Axon Guidance, Wnt signalling pathway, neurotrophin signalling pathway and focal adhesion. The 6 enriched KEGG pathways have all been previously reported to be related to OSCC^{11,15-18}.

Discussion

WGCNA is widely used in genomic data analysis, in which samples are independent of each other. In this paper, we modified the current WGCNA pipeline to analyse high-throughput genomic data from paired design. We demonstrated that it is feasible to construct co-expression networks using the Pearson correlation for paired data. To relate modules to phenotype, we used a linear mixed-effects model to account for the within-pair correlations. We calculated the gene significance of a node as the absolute value of the test statistic of the linear mixed effects model for testing the association of the node to the phenotype. We analysed the miRNA expression profile data

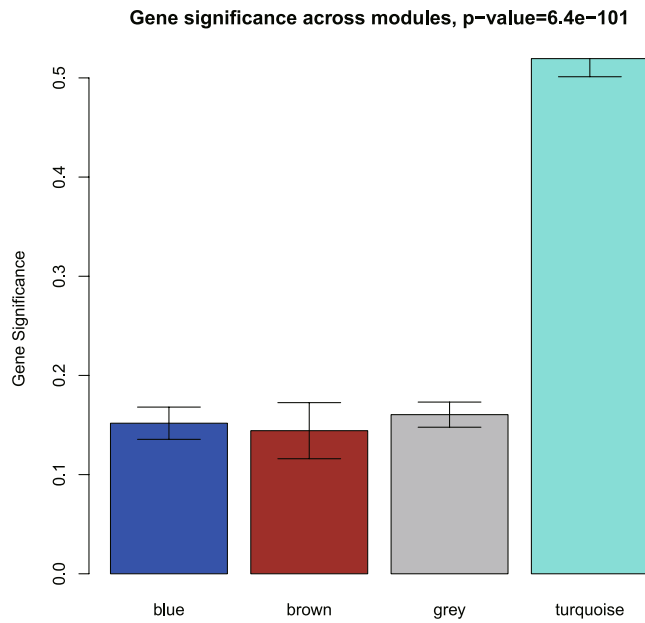


Figure 3. Barplot of module significance defined as the mean gene significance across all genes in the module.

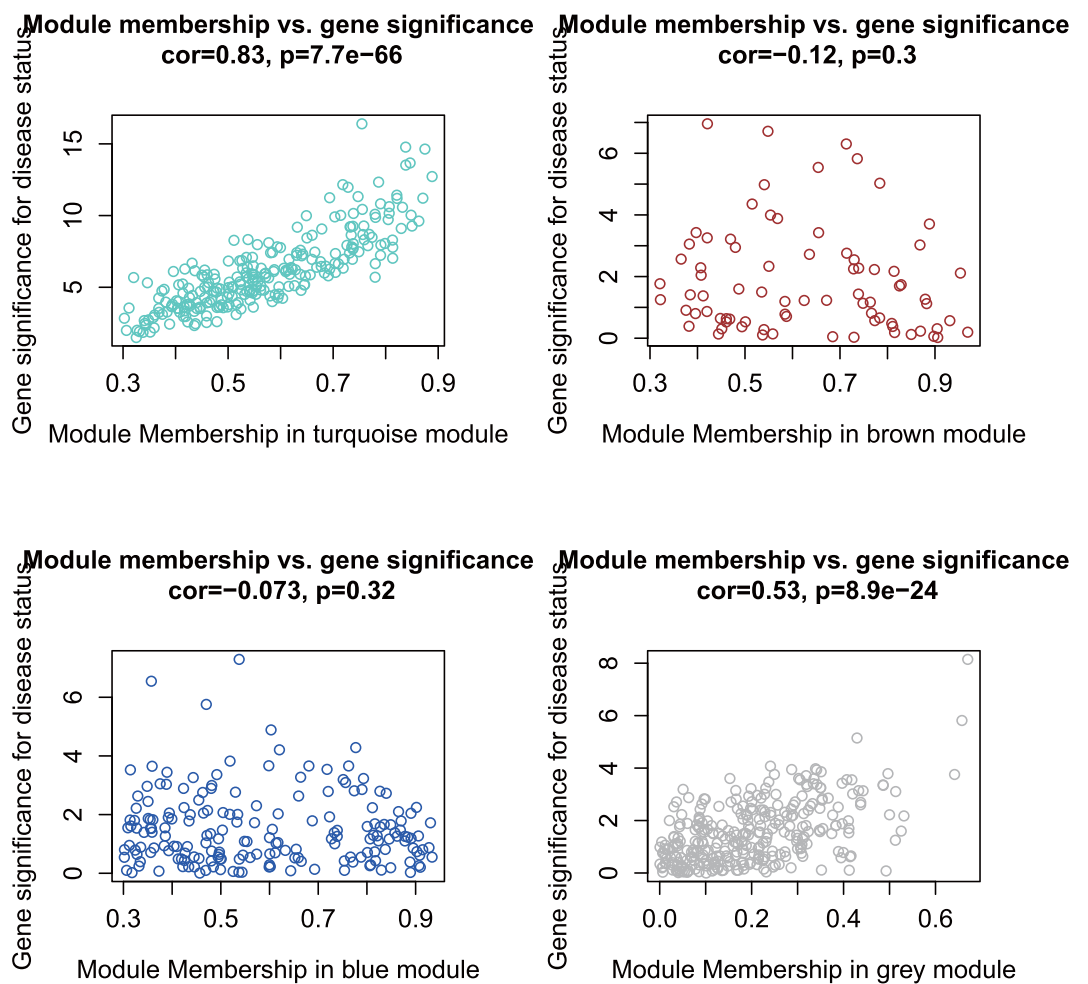


Figure 4. Correlation between MM and GS of all miRNAs in each module.

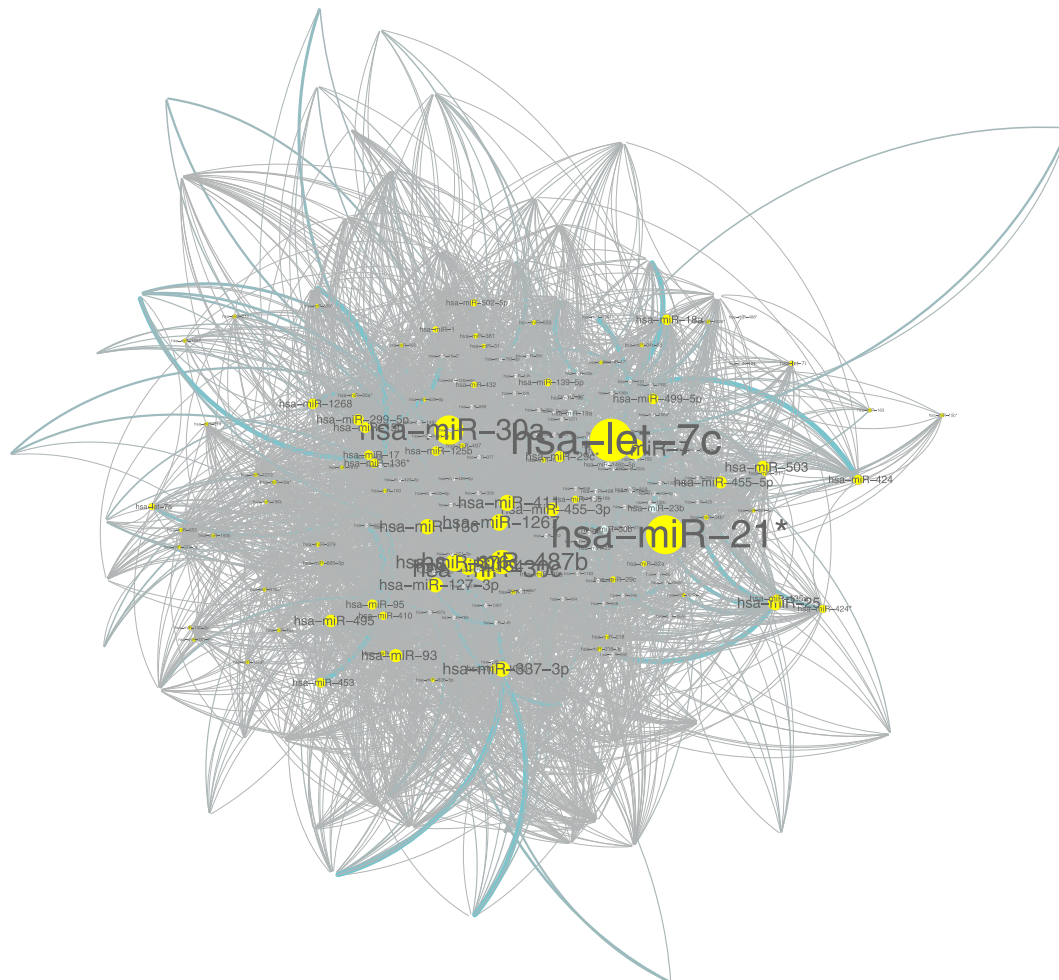


Figure 5. Network of miR-let-7 in the turquoise module.

miRNA	Gene Significance	Module Membership	Degree	Module
miR-let-7c	0.84	0.87	140	turquoise
miR-329	0.41	0.59	45	turquoise
miR-410	0.64	0.79	100	turquoise

Table 1. Network properties of miR-let-7c, miR-329 and miR-410.

(GSE45238) from a paired design study contributed to GEO by Shiah *et al.*¹¹ to illustrate the utility of the modified pipeline.

In this real data analysis, we identified one co-expression miRNA subnetwork (turquoise module) that was significantly associated with OSCC status and a set of OSCC-associated miRNAs (the grey module) that are not co-expressed among each other. The result of miRsystem showed that the top 6 enriched KEGG pathways for the two modules are the same and have all been previously reported to be related to OSCC^{11,15–18}. The turquoise module (with 254 miRNAs) contains most of the 84 miRNAs identified by the probe-wise approach in Shiah *et al.*¹¹. None of those 84 miRNAs are in the blue and brown modules that are not associated with OSCC. This is assuring and indicates that (1) most of the 84 miRNAs are in a co-expressed network and (2) more OSCC-related miRNAs could be found by using network approaches than by using the probe-wise approach.

In summary, the real data analysis showed that the modified WGCNA pipeline could identify biologically relevant modules. The limitations of our study include the small sample size and the lack of independent data to replicate our results. Further investigation is warranted.

This article demonstrated that miRNAs can form network modules that regulate human genes. It will be interesting to further investigate if the two detected miRNA modules may intertwine with other cellular networks. For instance, Tibiche and Wang (2008)¹⁹ showed that miRNAs preferentially regulate hub nodes and cut points of the network of metabolites, while avoiding regulating intermediate nodes.

It will also be interesting to investigate if miRNAs can be used to predict clinical outcomes, such as the risk of developing OSCC. It has been reported that highly connected network genes (i.e., hub genes) can correctly

classify tumour subtypes²⁰. To obtain better prediction performance, we can use both network hubs and network motifs, such as a positive regulatory loop²¹. To obtain robust (i.e., reproducible) prediction results, we can incorporate human signalling networks²², protein interaction networks²³ and gene ontology information²⁴ into the prediction process.

Methods

OSCC and microRNA. Oral squamous cell carcinomas (OSCC) is the sixth most common cancer worldwide. OSCC is the cause of over 400,000 cancer-related deaths each year, with 80 percent of deaths occurring in developing countries²⁵. Despite the progress made in OSCC treatment, the survival rate of patients after 5 years has not significantly improved due to late diagnosis, frequent loco-regional recurrences at the primary site and metastatic neck lymph nodes after treatment^{15,26}. MicroRNAs (miRNAs) are a kind of endogenous small length (22 nt) RNAs that have many important regulatory effects in the cell. Studies have shown that miRNAs are involved in the growth, differentiation, apoptosis, invasion, and metastasis of OSCC tumour cells²⁷. Shiah *et al.*¹¹ conducted a global microarray analysis of miRNA and detected eighty-four miRNAs differentially expressed in the OSCC specimens compared with the matched tissue. By using qRT-PCR and RT-PCR, these authors predicted two miRNAs, miR329 and miR410, that could potentially target Wnt-7b, an activator of the Wnt-b-catenin pathway, thereby attenuating the Wnt-b-catenin signalling pathway in OSCC. Importantly, the dysregulation of the Meg-3-miR329 and -410-Wnt-7b-b-catenin signalling axis may result from exposure to betel quid chewing. However, how miRNAs interplay with each other to contribute to the development of OSCC is still largely unknown. In this paper, we used WGCNA to detect OSCC-associated miRNA subnetworks (modules) based on the expression data of OSCC investigated by Shiah *et al.*¹¹.

Data. The data used in this paper was obtained from the GEO database in NCBI (Gene Expression Omnibus^{9,10}, <http://www.ncbi.nlm.nih.gov/geo/>), and the platform data entry number is GPL8179. The experimental data entry number is GSE45238. The dataset comes from the work of Shiah *S et al.*¹¹ in 2013. Forty OSCC specimens and their matched non-tumourous epithelial counterparts were selected in the dataset. There were 858 miRNAs in the dataset; we kept 830 miRNAs from Target Mature Version 12 for further analysis.

Constructing gene network. In the co-expression network of genes, nodes are genes, and edges indicate the magnitude of their co-expression. The variable x_i is denoted as the expression profile of the i -th gene, and WGCNA calculates the co-expression of genes based on an adjacency matrix. WGCNA defines the adjacency matrix based on co-expression similarity s_{ij} between the i -th gene and the j -th gene. By default, s_{ij} is defined as the absolute value of the Pearson correlation coefficient between the profiles of genes i and j ⁶:

$$s_{ij} = |cor(x_i, x_j)| \quad (1)$$

In statistics, the Pearson correlation is used to measure the linear correlation of two random variables. The Pearson correlation is also called inter-class correlation. Correspondingly, there is a concept called intra-class correlation in statistics, which was proposed to modify inter-class correlation to handle the case of paired measurements. It is natural to think that we should use intra-class correlation to measure the correlation between two genes when expression data are collected from paired design, in which the two samples within a pair are correlated. However, the intra-class correlation is not appropriate for measuring the correlation between two genes since it is used for repeated measurements of the same random variable in two correlated samples, not for two random variables (i.e., two genes). In this article, we showed that the Pearson correlation can be used to measure the magnitude of the co-expression of a pair of genes regardless of whether the data are from independent design or from paired design (See Supplementary Text). We showed

$$\begin{aligned} corr(Z_1, Z_2) &= \frac{Cov(Z_1, Z_2)}{\sqrt{Var(Z_1)Var(Z_2)}} \\ &= \frac{(1-p)Cov(X_1, X_2) + pCov(Y_1, Y_2) + p(1-p)\delta_1\delta_2}{\sqrt{[(1-p)\sigma_{X_1}^2 + p\sigma_{Y_1}^2 + p(1-p)\delta_1^2][(1-p)\sigma_{X_2}^2 + p\sigma_{Y_2}^2 + p(1-p)\delta_2^2]}} \end{aligned} \quad (2)$$

In Equation (2), $Z_i = (1 - \theta)X_i + \theta Y_i$ represents the expression level for the i -th gene, where θ indicates if the sample is from a case ($\theta = 1$) or from a control ($\theta = 0$), X_i is the expression level of the i -th gene for control tissue samples, and Y_i is the expression level of the i -th gene for tumour tissue samples. Equation (2) is true regardless of whether samples are paired or not, so the Pearson correlation between two genes is still valid for paired samples. Next, the co-expression similarity s_{ij} is transformed into the adjacency a_{ij} via an adjacency function²⁸:

$$a_{ij} = s_{ij}^\beta \quad (3)$$

where $\beta \geq 1$ is a soft threshold and is determined according to a scale-free topology criterion since the literature shows that most of the biological networks have the scale-free topology.

Detecting gene modules. A gene module is a cluster of densely interconnected genes in terms of co-expression. WGCNA uses hierarchical clustering to identify gene modules and colour to indicate modules. For genes that are not assigned to any of the modules, WGCNA places them in a grey module. That is, genes in the grey module are not co-expressed. The module eigengene (ME) of a module is defined as the first principal component of the module and represents the overall expression level of the module.

Detecting associations of modules to phenotype. To account for the within-pair correlation in data from paired design, the linear mixed-effects model (LMM) is used to test the association of a module to phenotype. In the OSCC data analysis, we used the following model for testing the association of a miRNA module to the tumour status (normal vs tumour):

$$y_{ij} = \beta_{0i} + \beta_1 \cdot tumour_j + \beta_2 \cdot age_i + \beta_3 \cdot stage_i + e_{ij} \quad i = 1, \dots, n, \quad j = 1, 2 \quad (4)$$

In the above model, y_{ij} is the expression level of the eigengene of the i -th subject for the j -th tissue sample. $j = 1$ indicates the control sample, and $j = 2$ indicates the tumour sample. $tumour_1 = 0$ indicates the control tissue, and $tumour_2 = 1$ indicates the tumour tissue. age_i is the age for the i -th subject. $stage_i$ is the tumor stage for the i -th subject. β_{0i} is the subject-specific random intercept to account for the within-pair correlation, and e_{ij} is the random error term. We assume $\beta_{0i} \sim N(\beta_0, \tau^2)$, $e_{ij} \sim N(0, \sigma^2)$, and β_{0i} and e_{ij} are mutually independent.

Another way to assess the association of a module to a phenotype in WGCNA is with the module significance (MS), which is defined as the average gene significance (GS) of all genes in the module. For data from paired design, the GS of a miRNA is defined as the absolute value of the test statistic of the linear mixed effects model for testing the association of the miRNA to the tumour status. By comparing the MS between modules, we can identify the modules that are highly related to the phenotype⁶.

Applying WGCNA to the OSCC data. We first used the R Bioconductor packages iCheck and lumi to draw the quantile plot and the scatter plot of principal components to check whether there were outlying probes, samples/arrays, and/or batch effects (Supplementary Figs 1 and 2). After data preprocessing, we repeated the principal component analysis to double check the data quality. No outlying probes were detected (Supplementary Fig. 3). We also observed that tumour samples and normal samples are separated in the PCA plot (Supplementary Fig. 4). Then, we performed hierarchical clustering on the samples to further detect potential outliers. We identified 2 outliers in the control group. We excluded these 2 control arrays and corresponding 2 matched tumour samples. The remaining 76 samples were used for further analysis (Supplementary Fig. 5). Next, we used R package WGCNA to perform the weighted correlation network analysis. We chose the soft threshold $\beta = 7$ to construct the co-expression network as the R^2 reached the peak for the first time when $\beta = 7$ (Supplementary Fig. 6). The plot of $\log_{10}(p(k))$ versus $\log_{10}(k)$ (Supplementary Fig. 7) indicates that by using $\beta = 7$, the network is close to a scale-free network, where k is the whole network connectivity and $p(k)$ is the corresponding frequency distribution. When $\beta = 7$, the R^2 is 0.98, ensuring that the network was close to the scale-free network. After the soft thresholding power β was determined, the Topological Overlap Matrix (TOM) (Supplementary Fig. 8) and $dissTOM = 1 - TOM$ were obtained. A hierarchical clustering of MEs was performed to study the correlations among the modules. To account for the within-pair correlation in data from paired design, we used the linear mixed-effects model (equation (4)) for testing the association of a module to the tumor status. We visualized the network that consists of the hub miR-let-7 and its connected nodes in the turquoise module by using Cytoscape²⁹, which is an open source software platform that is primarily used to visualize molecular interactions and biological pathways. In this study, we regarded a miRNA as the hub of a module if its degree (i.e., the number of edges) is the largest among all miRNAs in the module. For the grey module, we did not try to find a hub since miRNAs in this module are not co-expressed. To understand how miRNAs participate in the regulation of gene expression during pathogenic processes, it is useful to predict target genes and perform KEGG pathway enrichment analysis. In this study, the web tool miRsystem was used to predict the genes targeted by miRNAs. MiRsystem has integrated several prediction algorithms and experimentally validated data sources to reduce false positive predictions¹⁴.

Data availability. The datasets generated and/or analysed during the current study are available in the Gene Expression Omnibus (GEO) repository, <https://www.ncbi.nlm.nih.gov/geo/query/acc.cgi?acc=GSE45238>.

References

1. Arnone, M. I. & Davidson, E. H. The hardwiring of development: organization and function of genomic regulatory systems. *Development* **124**, 1851–1864 (1997).
2. Miklos, G. L. & Rubin, G. M. The Role of the Genome Project in Determining Gene Function: Insights from Model Organisms. *Cell* **86**, 521–529 (1996).
3. Chen, Y. *et al.* Variations in DNA elucidate molecular networks that cause disease. *Nature* **452**, 429–435 (2008).
4. Schadt, E. E. *et al.* An integrative genomics approach to infer causal associations between gene expression and disease. *Nature genetics* **37**, 710–717 (2005).
5. Stuart, J. M., Segal, E., Koller, D. & Kim, S. K. A Gene-Coexpression Network for Global Discovery of Conserved Genetic Modules. *Science* **302**, 249–255 (2003).
6. Langfelder, P. & Horvath, S. WGCNA: an R package for weighted correlation network analysis. *BMC bioinformatics* **9**, 559 (2008).
7. Zhang, B. & Horvath, S. A General Framework For Weighted Gene Co-Expression Network Analysis. *Statistical Applications in Genetics Molecular Biology* **4**, Article 17 (2005).
8. Fuller, T. F. *et al.* Weighted gene coexpression network analysis strategies applied to mouse weight. *Mammalian Genome* **18**, 463–472 (2007).
9. Edgar, R., Domrachev, M. & Lash, A. E. Gene Expression Omnibus: NCBI gene expression and hybridization array data repository. *Nucleic Acids Research* **30**, 207–210 (2002).
10. Barrett, T. *et al.* NCBI GEO: archive for functional genomics data sets-update. *Nucleic Acids Research* **41**, D991–D995 (2013).
11. Shiah, S.-G. *et al.* Downregulated miR329 and miR410 promote the proliferation and invasion of oral squamous cell carcinoma by targeting Wnt-7b. *Cancer Research* **74**, 7560–7572 (2014).
12. Manikandan, M. *et al.* Oral squamous cell carcinoma: microRNA expression profiling and integrative analyses for elucidation of tumorigenesis mechanism. *Molecular Cancer* **15**, 28 (2016).
13. Hui, A. B. *et al.* Comprehensive MicroRNA profiling for head and neck squamous cell carcinomas. *Clinical Cancer Research* **16**, 1129–1139 (2010).

14. Lu, T.-P. *et al.* miRsystem: an integrated system for characterizing enriched functions and pathways of microRNA targets. *PLoS ONE* **7**, e42390 (2012).
15. Sticht, C. *et al.* Activation of MAP kinase signaling through ERK5 but not ERK1 expression is associated with lymph node metastases in oral squamous cell carcinoma (OSCC). *Neoplasia* **10**, 462–470 (2008).
16. Ge, L. *et al.* Differential mRNA expression profiling of oral squamous cell carcinoma by high-throughput RNA sequencing. *Journal of Biomedical Research* **29**, 397–404 (2015).
17. Zhou, Y., Kolokythas, A., Schwartz, J. L., Epstein, J. B. & Adami, G. R. microRNA from brush biopsy to characterize oral squamous cell carcinoma epithelium. *Cancer Medicine* **6**, 67–78 (2017).
18. India Project Team Of The International Cancer Genome Consortium *et al.* Mutational landscape of gingivo-buccal oral squamous cell carcinoma reveals new recurrently-mutated genes and molecular subgroups. *Nature Communications* **4**, 2873 (2013).
19. Tibiche, C. & Wang, E. MicroRNA Regulatory Patterns on the Human Metabolic Network. *Open Systems Biology Journal* **1**, 1–8 (2008).
20. Zaman, N. *et al.* Signaling Network Assessment of Mutations and Copy Number Variations Predict Breast Cancer Subtype-Specific Drug Targets. *Cell Reports* **5**, 216–223 (2013).
21. McGee, S. R., Tibiche, C., Trifiro, M. & Wang, E. Network Analysis Reveals A Signaling Regulatory Loop in the PIK3CA-mutated Breast Cancer Predicting Survival Outcome. *Genomics, Proteomics & Bioinformatics* **15**, 121–129 (2017). Biomarkers for Human Diseases and Translational Medicine.
22. Fu, C., Li, J. & Wang, E. Signaling network analysis of ubiquitin-mediated proteins suggests correlations between the 26S proteasome and tumor progression. *Molecular Biosystems* **5**, 1809–1816 (2009).
23. Wang, E. Understanding genomic alterations in cancer genomes using an integrative network approach. *Cancer Letters* **340**, 261–269 (2013).
24. Gao, S. *et al.* Identification and Construction of Combinatory Cancer Hallmark-Based Gene Signature Sets to Predict Recurrence and Chemotherapy Benefit in Stage II Colorectal Cancer. *JAMA Oncology* **2**, 37–45 (2016).
25. Pisani, P., Parkin, D. & Ferlay, J. Estimates of the worldwide mortality from eighteen major cancers in 1985. Implications for prevention and projections of future burden. *International Journal of Cancer* **55**, 891–903 (1993).
26. Shenouda, S. K. & Alahari, S. K. MicroRNA function in cancer: oncogene or a tumor suppressor? *Cancer and Metastasis Reviews* **28**, 369–378 (2009).
27. Bidaud, P. *et al.* Expression of p53 family members and CD44 in oral squamous cell carcinoma (OSCC) in relation to tumorigenesis. *Histology and Histopathology* **25**, 331–339 (2010).
28. Horvath, S. *et al.* Analysis of oncogenic signaling networks in glioblastoma identifies ASPM as a molecular target. *Proceedings of the National Academy of Sciences* **103**, 17402–17407 (2006).
29. Shannon, P. *et al.* Cytoscape: a software environment for integrated models of biomolecular interaction networks. *Genome Research* **13**, 2498–2504 (2003).

Acknowledgements

This work was supported by the Beijing Natural Science Foundation (4152007) and China National Key Technology Research and Development Program project with no. 2015BAH13F01.

Author Contributions

Shi Chen and Hui Pan analysed the results; Jianqiang Li, Doudou Zhou, Qing Wang and Yuliang Shi analysed the data; and Jianqiang Li, Ji-Jiang Yang, and Weiliang Qiu proposed and directed this research. All authors reviewed the manuscript.

Additional Information

Supplementary information accompanies this paper at <https://doi.org/10.1038/s41598-017-18705-z>.

Competing Interests: The authors declare that they have no competing interests.

Publisher's note: Springer Nature remains neutral with regard to jurisdictional claims in published maps and institutional affiliations.



Open Access This article is licensed under a Creative Commons Attribution 4.0 International License, which permits use, sharing, adaptation, distribution and reproduction in any medium or format, as long as you give appropriate credit to the original author(s) and the source, provide a link to the Creative Commons license, and indicate if changes were made. The images or other third party material in this article are included in the article's Creative Commons license, unless indicated otherwise in a credit line to the material. If material is not included in the article's Creative Commons license and your intended use is not permitted by statutory regulation or exceeds the permitted use, you will need to obtain permission directly from the copyright holder. To view a copy of this license, visit <http://creativecommons.org/licenses/by/4.0/>.

© The Author(s) 2018